Volume 52
Number 19
21 May 2023
Pages 6197-6590

Dalton Transactions

An international journal of inorganic chemistry

rsc.li/dalton

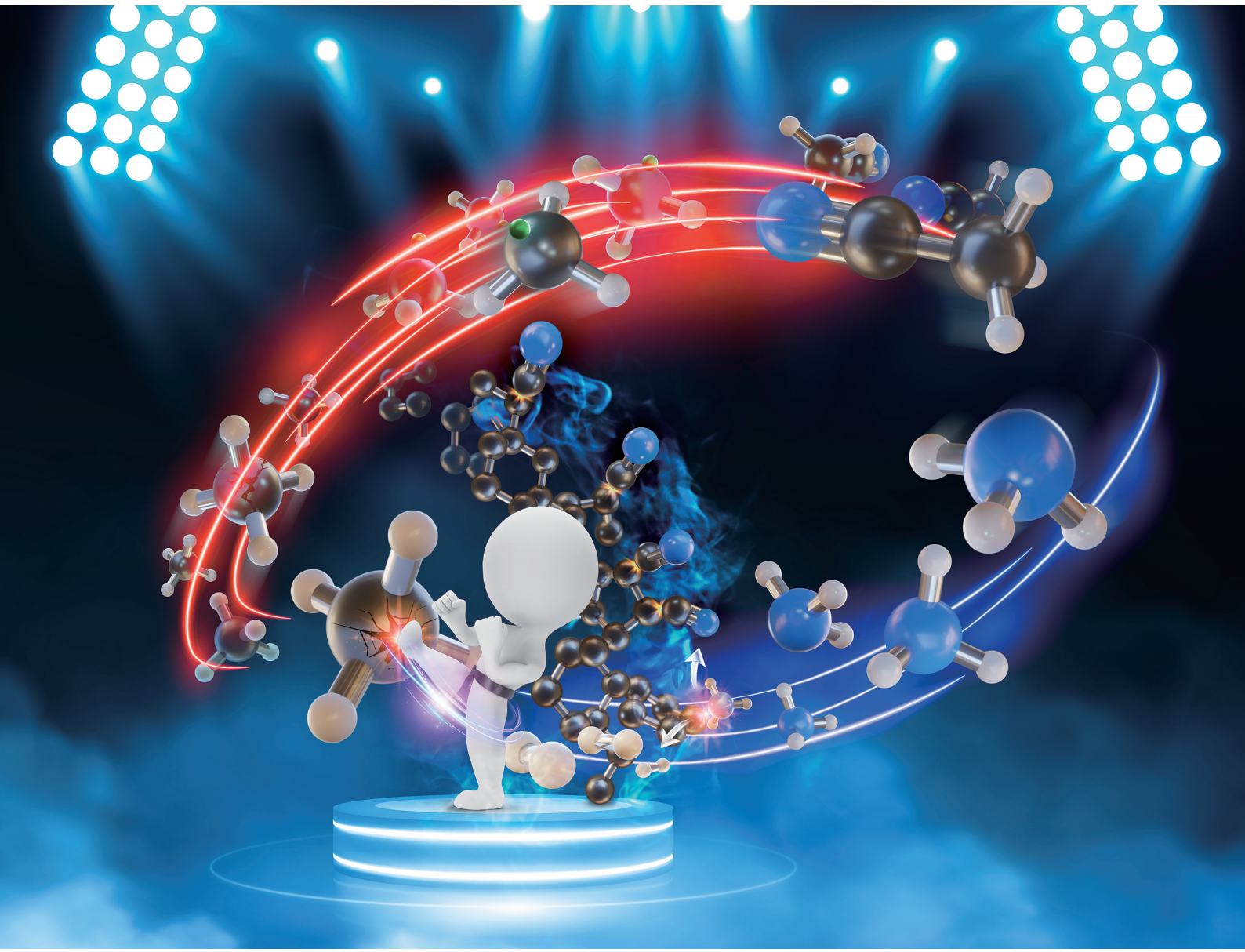

ISSN 1477-9226

ROYAL SOCIETY OF CHEMISTRY

PERSPECTIVE

Korawich Trangwachirachai and Yu-Chuan Lin

Light hydrocarbon conversion to acrylonitrile and acetonitrile – a review

Dalton Transactions

ROYAL SOCIETY OF CHEMISTRY

PERSPECTIVE

View Article Online
View Journal | View Issue

Check for updates

Cite this: *Dalton Trans.*, 2023, **52**, 6211

Light hydrocarbon conversion to acrylonitrile and acetonitrile – a review

Korawich Trangwachirachai and Yu-Chuan Lin *

Received 25th November 2022,
Accepted 22nd February 2023

DOI: 10.1039/d2dt03795e

rsc.li/dalton

Nitriles, particularly acrylonitrile and acetonitrile, are versatile chemicals that are used in various fields, such as polymer synthesis and pharmaceutical production. For a long time, acrylonitrile has been produced *via* propylene ammoxidation with acetonitrile as a byproduct. The depletion of crude reservoirs and the production of unconventional hydrocarbon resources (*e.g.*, shale gas) renders light alkanes (including propane, ethane, and methane) to be potential feedstocks in the syntheses of acrylonitrile and acetonitrile. In this review, the processes of transforming light hydrocarbons to nitriles are surveyed, the developments in nitrile synthesis from alkanes are discussed, and the existing challenges and plausible solutions are addressed.

Published on 22 February 2023. Downloaded by Yunnan University on 8/24/2025 1:45:34 PM.

1. Introduction

Acrylonitrile (AN) and acetonitrile (ACN) are useful chemicals widely used in the chemical industry.[1] AN, alias 2-propenenitrile, propylene nitrile, and vinyl cyanide,[2] has its chemical formula of C_3H_3N with the structure of $CH_2{=}CH{-}C{\equiv}N$. It is a colorless liquid at ambient conditions. The presence of a conjugated nitrile functional group with a carbon–carbon double bond makes AN a polar compound. AN is used in polymerization to form polymers,[3–5] and in hydration with sulfuric acid to form acrylamide sulfate ($C_3H_5NO{\cdot}H_2SO_4$).[6,7] Acrylamide sulfate can be converted to acrylamide (C_3H_5NO) by base-neutralization, and the hydration of acrylamide yields acrylic acid. Catalytic partial hydration of AN by copper-based catalysts can also produce acrylamide.[8–11] Other applications of AN have been reported, such as Diels–Alder addition to dienes to form cyclic compounds, hydrogenation to synthesize propionitrile (C_3H_5N) and propylamine (C_3H_9N), and hydrodimerization to prepare adiponitrile ($C_6H_8N_2$).[12,13]

ACN, also called methyl cyanide, is a saturated aliphatic nitrile with a chemical formula of C_2H_3N and the structure of

Department of Chemical Engineering, National Cheng Kung University, Tainan 70101, Taiwan. E-mail: yclin768@mail.ncku.edu.tw

Korawich Trangwachirachai

Korawich Trangwachirachai was born in Bangkok, Thailand. He earned his bachelor's (2015) and master's degrees (2018) in the Department of Chemistry, King Mongkut's Institute of Technology Ladkrabang, Thailand. His previous research mainly focused on dehydrogenation of propane to propylene and non-oxidative methane coupling. He is studying for a Ph.D. in Chemical Engineering at National Cheng Kung University, Taiwan. Currently, his research mainly focuses on the synthesis of acetonitrile from methane using heterogeneous catalysis approaches.

Yu-Chuan Lin

Yu-Chuan Lin received his BS (2000) and MS (2002) degrees from National Cheng Kung University (NCKU) and then conducted his Ph.D. study on catalytic partial oxidation at Kansas State University. After obtaining his Ph.D. degree (2006), Yu-Chuan held postdoctoral positions at Academia Sinica (2006–07) and the University of Massachusetts-Amherst (2007–2008), both focusing on biomass conversion. In 2009, he served as an Assistant Professor at Yuan Ze University (Taiwan). He returned to NCKU (2014) where he was promoted to Associate Professor (2018) and to Professor (2022). Yu-Chuan's research focuses on designing heterogeneous catalysts in pursuit of two thrusts: energy applications and waste utilization.

Published on 22 February 2023. Downloaded by Yunnan University on 8/24/2025 1:45:34 PM.

CH_3–C≡N. ACN exhibits excellent solubility to both polar and non-polar compounds with a low freezing point, low toxicity, and low viscosity.[14] It is widely used as a solvent and reactant in organic synthesis, a mobile phase in high-performance liquid chromatography, and an extractor of butadiene for the hydrocarbons stream.[1,15,16] ACN can co-react with methane or methanol to produce AN.[17]

Currently, the commercial route of ACN synthesis is absent. ACN is a byproduct, with approximately 2–4% yield, in the AN synthesis. Propylene ammoxidation (also called the Sohio process) is the existing route in AN production. AN can also be produced by the ethylene cyanohydrin (C_3H_5NO) process.[18,19] The ethylene cyanohydrin process involves co-reacting ethylene oxide and hydrogen cyanide (HCN) to generate ethylene cyanohydrin, followed by the dehydration of ethylene cyanohydrin to form AN by using diethylamine as a base catalyst. AN was also commercially synthesized by the addition of HCN to acetylene using cuprous chloride in a dilute HCl solution.[20] Other methods were reported, such as HCN addition to acetaldehyde,[21] dehydrogenation of propionitrile,[22,23] coupling of propylene and nitric oxide,[24,25] and dehydration of acrylamide.[2] However, these processes are not commercialized.

Recently, the ammoxidation of ethanol to ACN has drawn attention due to its high atomic efficiency.[14,26] TiO_2 and ZrO_2 supported vanadium oxide catalysts were tested for this reaction. V_2O_5/ZrO_2 showed a complete ethanol and oxygen conversion with a selectivity of 70% and 20% for ACN and CO_x, respectively, at 400 °C.[27] Kinetic parameters were also analyzed.[26] The acidity of vanadium-based catalysts is a major difficulty in ethanol ammoxidation because it leads to a dehydration of ethanol.[28] Disadvantages include a high ammonia-to-feed ratio and the inevitable generation of hazardous HCN, raising concerns about the environmental impact.[28–31]

C_{1-3} hydrocarbons were produced from the steam cracking process with approximately 65.7% yield.[32] Owing to the shale gas revolution,[33] production of light hydrocarbons is growing steadily.[34,35] Such a growing trend creates a niche for transforming light hydrocarbons into value-added chemicals. Fig. 1 shows the average price of each chemical in the USA in 2017.[36] The prices of ACN and AN are much higher than those of light hydrocarbons, especially alkanes. Hence, converting those light hydrocarbons into ACN or AN shall be value-added processes. Herein, this review focuses on the synthesis of nitriles, particularly AN and ACN, from light hydrocarbons, including propylene, propane, ethylene, ethane, and methane. The chemistry of each reaction is discussed. This review also addresses recent studies from the last 5 years and the remaining challenges for the conversion of light hydrocarbons to nitriles.

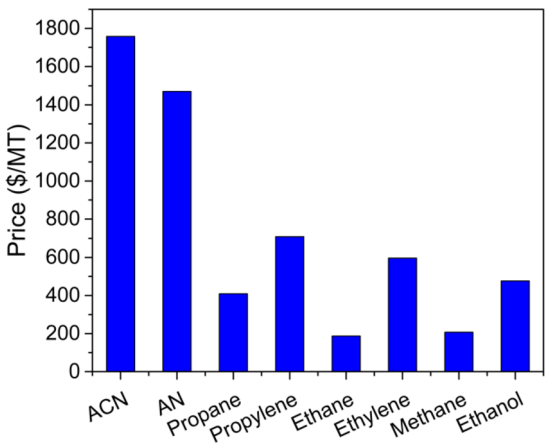

Fig. 1 Market price of light alkanes, ethanol, ACN, and AN in USA, 2017.[36]

2. Chemistry of nitriles synthesis from C_3 and C_2 hydrocarbons

2.1 Ammodehydrogenation

Ammodehydrogenation transforms a hydrocarbon reactant to a nitrogen-containing product in an oxygen-free environment by using gaseous ammonia as the nitrogen donor. Propylene ammodehydrogenation has been reported to generate propionitrile and hydrogen, as shown in eqn (1).[37]

$$C_3H_6 + NH_3 \rightarrow C_3H_5N + 2H_2 \quad \Delta H^\circ = 77.1 \text{ kJ mol}^{-1} \quad (1)$$

The produced propionitrile could be further dissociated to form ACN and methane by hydrogenolysis (eqn (2)).

$$C_3H_5N + H_2 \rightarrow C_2H_3N + CH_4 \quad \Delta H^\circ = -38.5 \text{ kJ mol}^{-1} \quad (2)$$

Therefore, by adding eqn (1) and (2), the overall reaction of propylene ammodehydrogenation to produce ACN can be expressed as

$$C_3H_6 + NH_3 \rightarrow C_2H_3N + CH_4 + H_2 \quad \Delta H^\circ = 38.6 \text{ kJ mol}^{-1} \quad (3)$$

ACN can also be produced from the ammodehydrogenation of ethane and ethylene, shown in eqn (4) and (5).[38]

$$C_2H_6 + NH_3 \rightarrow C_2H_3N + 3H_2 \quad \Delta H^\circ = 218.6 \text{ kJ mol}^{-1} \quad (4)$$

$$C_2H_4 + NH_3 \rightarrow C_2H_3N + 2H_2 \quad \Delta H^\circ = 81.7 \text{ kJ mol}^{-1} \quad (5)$$

Ammodehydrogenation of ethane and ethylene are energy-demanding, endothermic reactions. Moreover, polycondensation of propylene and ethylene for coke formation can be facilitated at high temperatures. Accordingly, controlling the feeding ratio of reactants and diluent is important to suppress the extent of coking.

2.2 Ammoxidation

Ammoxidation converts the hydrocarbon reactant with oxygen and gaseous ammonia to yield a nitrile. For instance, AN can be produced from propane and propylene by ammoxidation, as shown in eqn (6) and (7).[39,40]

$$C_3H_8 + NH_3 + 2O_2 \rightarrow C_3H_3N + 4H_2O \quad \Delta H^\circ = -637.6 \text{ kJ mol}^{-1} \quad (6)$$

This journal is © The Royal Society of Chemistry 2023

Published on 22 February 2023. Downloaded by Yunnan University on 8/24/2025 1:45:34 PM.

$$C_3H_6 + NH_3 + 3/2O_2 \rightarrow C_3H_3N + 3H_2O \quad \Delta H^\circ = -520.1 \text{ kJ mol}^{-1} \quad (7)$$

ACN can be derived from propane and propylene ammoxidation through C–C cleavage to produce HCN (eqn (8) and (9)).[41]

$$C_3H_8 + 2NH_3 + 5/2O_2 \rightarrow C_2H_3N + HCN + 5H_2O \quad \Delta H^\circ = -794.5 \text{ kJ mol}^{-1} \quad (8)$$

$$C_3H_6 + 2NH_3 + 2O_2 \rightarrow C_2H_3N + HCN + 4H_2O \quad \Delta H^\circ = -676.9 \text{ kJ mol}^{-1} \quad (9)$$

Because of the same carbon number, ammoxidation of ethane and ethylene allows ACN to be produced from the ammoxidation of ethane or ethylene without a loss of a carbon atom, as shown in eqn (10) and (11).[42,43]

$$C_2H_6 + NH_3 + 3/2O_2 \rightarrow C_2H_3N + 3H_2O \quad \Delta H^\circ = -506.8 \text{ kJ mol}^{-1} \quad (10)$$

$$C_2H_4 + NH_3 + O_2 \rightarrow C_2H_3N + 2H_2O \quad \Delta H^\circ = -401.9 \text{ kJ mol}^{-1} \quad (11)$$

Alkenes (propylene and ethylene) were intermediates in the alkane (propane and ethane) ammoxidation. Hence, oxidative dehydrogenation of alkanes to alkenes may occur, as shown in eqn (12) and (13).[44,45]

$$C_3H_8 + \frac{1}{2}O_2 \rightarrow C_3H_6 + H_2O \quad \Delta H^\circ = -117.5 \text{ kJ mol}^{-1} \quad (12)$$

$$C_2H_6 + \frac{1}{2}O_2 \rightarrow C_2H_4 + H_2O \quad \Delta H^\circ = -104.9 \text{ kJ mol}^{-1} \quad (13)$$

Both ammoxidation and oxidative dehydrogenation are exothermic, which can be operated at lower temperatures than those of the endothermic ammodehydrogenations. However, the undesired overoxidation of reactants and products to form carbon oxides and nitrogen oxides is frequently encountered in ammoxidation. Therefore, precisely controlling the amount of fed oxygen is the key to elevating the product yield.

2.3 Thermodynamics

Thermodynamic analysis can provide information on reaction conditions that are proper for the ammodehydrogenation and ammoxidation of C_3 and C_2 hydrocarbons to yield AN and ACN. Fig. 2 shows $\Delta G_r/RT$ as a function of temperature for the syntheses of AN (Fig. 2a) and ACN (Fig. 2b).

Ammoxidation shows an upward-converging trend while ammodehydrogenation exhibits a downward-converging trend, underlining their exothermic and endothermic nature. All ammoxidation routes are thermodynamically feasible in the range of 300–1000 K. However, the ammodehydrogenation of propylene is favorable at $T > 400$ K (purple curve in Fig. 2b), while the ammodehydrogenations of ethane (green curve) and ethylene (navy curve) are thermodynamically unfavorable. Although thermodynamically unfavorable, non-oxidative synthesis of ACN from ethane and ethylene has been reported.[38]

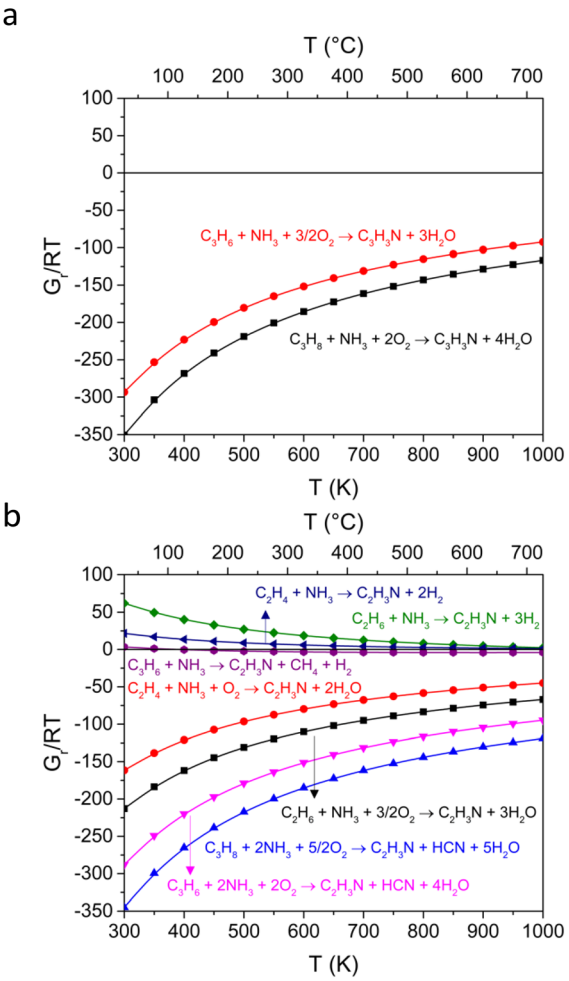

Fig. 2 Thermodynamic evaluation of the syntheses of (a) AN and (b) ACN.

It should be noted that thermodynamics only provides the theoretically calculated results of the equilibrium state. In general, increasing the reaction temperature allows the reaction rate to be enhanced even for exothermic reactions, known as the Polanyi–Wigner relation.[46] Catalyst design is thereby crucial to promote the rate by creating new paths that have a lower activation barrier of the desired reaction.

3. Synthesis of nitriles

3.1 Ammoxidation of propylene and propane

Back in the 1950s, non-oxidative synthesis of ACN in ammonia vapor (ammodehydrogenation) was tested by using C_3–C_5 olefins ($C_{3-5}^{=}$) as the feedstocks.[37] A silica-based material containing 4 wt% of alumina and 10 wt% of zirconia was used as the catalyst. The reaction temperature was in the range of 480–760 °C; pressure, 1–17 atm; ammonia-to-olefin ratio, 1 : 1 to 8 : 1. Among $C_{3-5}^{=}$, propylene can be converted to ACN under the mildest conditions (T = 640 °C, P = 1 atm, and ammonia-to-olefin ratio of 3 : 1) with a 9 mol% yield of ACN by propylene

Published on 22 February 2023. Downloaded by Yunnan University on 8/24/2025 1:45:34 PM.

bases. Denton *et al.*[47] proposed the reaction route of ACN production from propylene ammodehydrogenation to be a two-step process: (i) propylene reacts with ammonia to form propionitrile (eqn (1)), following by (ii) propionitrile dissociation to yield ACN and methane by hydrogenolysis (eqn (2)). The first reaction was validated by using a nickel catalyst at 345 °C. The obtained product was mainly propionitrile with a small amount of ACN. The second reaction was tested by converting propionitrile at 525 °C. Approximately 20% of propionitrile was transformed into ACN together with condensed compounds, gas, and coke. This emphasized that propionitrile is an intermediate in the conversion of propylene to ACN. Nevertheless, the operating temperature was typically higher than 525 °C for non-oxidative operations. This urges the development of oxidative conversion of propylene to ACN (ammoxidation) with lower energy demand.

Propylene ammoxidation was inspired by the selective oxidation of hydrocarbons by using oxides containing lattice oxygen.[48] Acrolein (C_3H_4O) could be successfully synthesized from the partial oxidation of propylene and oxygen over a SiO_2-supported bismuth-phosphomolybdate (BiPMo) catalyst. The metal ion of the oxide (herein Mo) should be at a higher oxidation state, allowing propylene to be partially oxidized to acrolein by lattice oxygen and leaving the metal ion of the oxide to have a lower oxidation state (reduced form). A zero-order kinetics was observed with respect to the oxygen partial pressure. That is, the catalyst surface was saturated with active oxygens to participate in partial oxidation. The reduced oxide can be re-oxidized by calcination.[49]

With the discovery of the BiPMo catalyst in propylene conversion to acrolein, transforming acrolein into nitrogen-containing compounds had been explored. Catalytic ammoxidation was operated by passing a mixture of propylene, ammonia, and air (molar ratio = 1 : 1.1 : 13.1) through a fluidized-bed reactor loaded with a BiPMo catalyst (see eqn (7)).[39,40] The benchmark reaction was conducted at 470 °C under atmospheric pressure with a contact time of 9.1 s. More than 95% of propylene could be converted with only 22.3% of carbon oxides. Nitrogen-containing products including AN, ACN, and hydrogen cyanide (HCN) were observed. However, the major product was AN (65.2%), while the ACN yield was only 4.0%. This is because the C=C bond of AN must be cleaved *via* hydrogenolysis to produce ACN. Moreover, ammoxidation is exothermic and is preferred in a low-temperature operation. This process is called the Sohio process, which has been industrially practiced for more than 60 years.

The mechanism of propylene ammoxidation was investigated by using deuterium labeling propylene (CH_2=CH–CH_2D).[50–54] The first-order kinetics was observed with respect to the partial pressure of propylene; zero-order kinetics, oxygen and ammonia pressures. Therefore, the C–H bond activation of the methyl group of propylene, forming a symmetrical allyl alkoxide intermediate, is proposed to be rate-limiting (see Fig. 3). This implied that acrolein and AN originated from the same intermediate. However, with the presence of ammonia, the allyl alkoxide tends to react with ammonia to

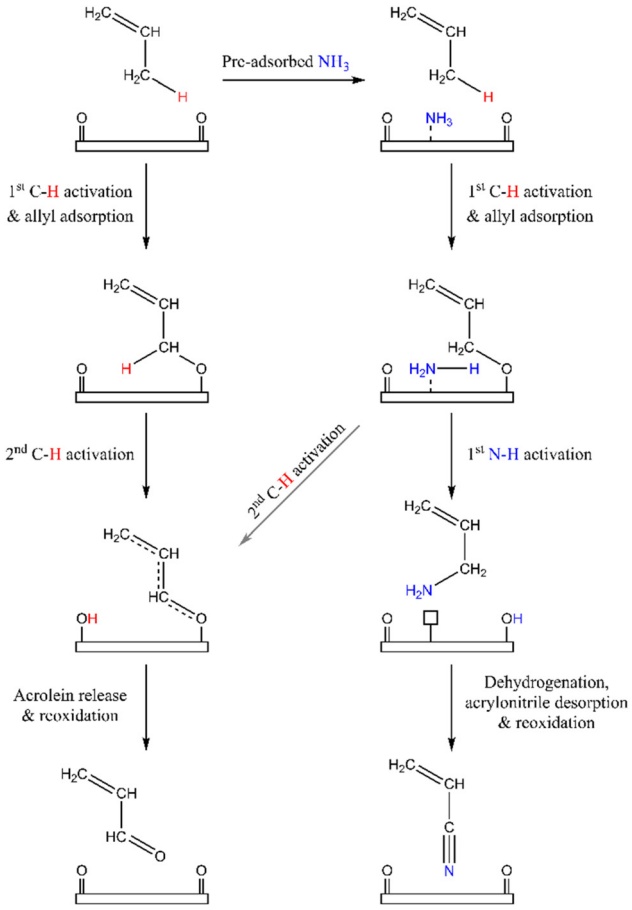

Fig. 3 Mechanism of propylene oxidation and ammoxidation. Adapted with permission.[41,49] Copyright 1970, American Chemical Society; 2021, Elsevier Inc.

produce AN rather than the abstraction of its α-hydrogen to form acrolein.[41] Accordingly, this discovery opens an alternative route to produce AN and ACN from propane.

AN can be produced from propane *via* two routes.[55] The first route is a sequential reaction, including a dehydrogenation of propane to propylene before propylene ammoxidation; the second route, a direct ammoxidation of propane to AN (see eqn (6)). The latter route was more attractive because the production cost could be reduced by approximately 15–20% compared to the former.[56]

In the 1970s, a number of inventions in propane ammoxidation were reported. Mo-based mixed oxides were frequently used as catalysts, similar to those utilized in propylene ammoxidation. The propane ammoxidation was mostly conducted at 550 °C. However, low propane conversion (29 mol%) and AN selectivity (15 mol%) were obtained.[57] Both propane conversion and AN selectivity can be improved by adding a gas phase additive. Tullman[58] reported that a high propane conversion (>90%) and AN yield (>60%) could be obtained when co-feeding CH_3Br in propane ammoxidation by using Mo-based catalysts. The CH_3Br additive is proposed to be an initiator, which is active for hydrogen abstraction from the

 This journal is © The Royal Society of Chemistry 2023

Published on 22 February 2023. Downloaded by Yunnan University on 8/24/2025 1:45:34 PM.

paraffinic C–H bond. Although the propane conversion and AN yield could be improved, the presence of the additive could facilitate catalyst poisoning and reactor corrosion.

In the 1980s, scheelite-type Bi–V–Mo-based catalysts[59–61] and rutile-type Sb–V-based catalysts[62–64] were applied for propane ammoxidation without co-feeding additives by BP/Sohio. For Bi–V–Mo catalysts, the operating temperature for propane ammoxidation could be reduced to 470 °C with a contact time of 1.5 s using a mixture of propane, ammonia, oxygen, and water (molar ratio = 5 : 1 : 2 : 1). A high selectivity of AN (61%) could be obtained. However, the propane conversion was only 12%. For Sb–V catalysts, propane ammoxidation was conducted at 500 °C with a 4.5 s contact time. Mixed reagents including propane, ammonia, oxygen, nitrogen, and water (molar ratio = 1 : 2 : 2 : 7.5 : 3) were used, and a propane conversion of 67% and an AN yield of 40% were obtained.

The Sb/V ratio, reaction pathway, and kinetics of propane ammoxidation were studied.[56] The Sb/V ratio should be higher than unity to obtain a high AN selectivity. High selectivity of propylene was observed at low propane conversion and was decreased with increasing propane conversion. ACN selectivity showed a trend similar to that of propylene. In contrast, the carbon oxides selectivity increased with enhanced propane conversion. The selectivity trend of AN was peculiar. It first increased, and then decreased with its maximal at approximately 30% propane conversion. These variations of product selectivity suggested that propylene is an intermediate in propane ammoxidation.

The kinetics study of propane ammoxidation was divided into two parts, *i.e.*, dehydrogenation of propane to propylene and ammoxidation of propylene to nitriles (AN and ACN). For propylene formation, the first-order rate expression with respect to the partial pressure of propane was observed. A Langmuir–Hinshelwood (LH) formalism was established regarding oxygen and ammonia partial pressures, in which the propylene production rate had almost no change at high ammonia partial pressure. The kinetic analysis implied that propylene is formed on the catalyst surface through which the adsorption of propane is rate-limiting. The LH-type formalism of nitriles formation was observed depending on propane and oxygen partial pressures, suggesting that nitriles are not directly formed from propane, but formed from adsorbed intermediate evolving from propylene. The partial pressure of water had almost no effect on both propylene and nitriles production rates, indicating that water acts as a bystander.

Albonetti *et al.* investigated the mechanism of propane ammoxidation and oxidation.[65] They discovered that ammonia had no effect on enhancing propane conversion and propylene yields. Thus, AN is proposed to be generated by the reaction of ammonia with oxygenate intermediates (*e.g.*, acrolein and allyl alkoxide species). The improved AN yield with increasing oxygen partial pressure further supported this claim. Moreover, propylene is verified as the precursor of AN. Guerrero-Pérez *et al.* used a rapid-scan FTIR equipped with a mass spectrometer to elucidate the mechanism of propane ammoxidation and oxidation reactions.[66] They found that the oxygenates were not formed at the outset of the reaction. They stated that propylene promptly evolved from propane, and oxygenates may be produced by the subsequent reactions (*e.g.*, propylene ammoxidation to AN).

Propane ammoxidation requires a multifunctional catalyst. Therefore, MoVTeNb mixed metal oxides were developed.[68] A 76% propane conversion was obtained with 66% AN selectivity at 420 °C by using $Mo_1V_{0.4}Te_{0.2}Nb_{0.1}O_x$ catalyst. The outstanding performance could be attributed to its unique structure. It contains three major phases, including orthorhombic $Mo_{7.5}V_{1.5}TeNbO_{29}$ (M1), pseudohexagonal $Mo_6VTe_2O_{24}$ (M2), and monoclinic Mo_5TeO_{16} (M3), in which the M1 phase is the most crucial. The M1 phase consists of all catalytic centers (see, Fig. 4), where the C–H bond is activated by a V^{5+} site, α-hydrogen abstraction of allylic species by a Te^{4+} site, and an N-insertion by a Mo^{6+} site.[67] Moreover, it was found that the AN yield could be improved with a higher extent of the M1 phase (Fig. 5). Therefore, the mechanism of propane ammoxi-

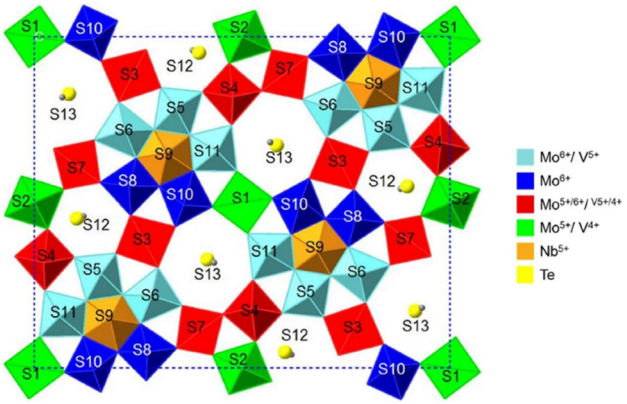

Fig. 4 Representation of the M1 phase viewed along the *c*-axis direction with 13 cation sites. Reproduced with permission.[67] Copyright 2020, Springer Nature.

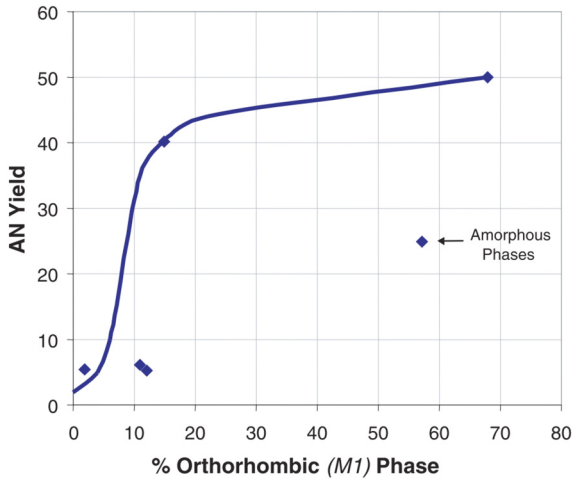

Fig. 5 Acrylonitrile yield *versus* % M1 phase. Reproduced with permission.[68] Copyright 2003, Plenum Publishing Corporation.

Published on 22 February 2023. Downloaded by Yunnan University on 8/24/2025 1:45:34 PM.

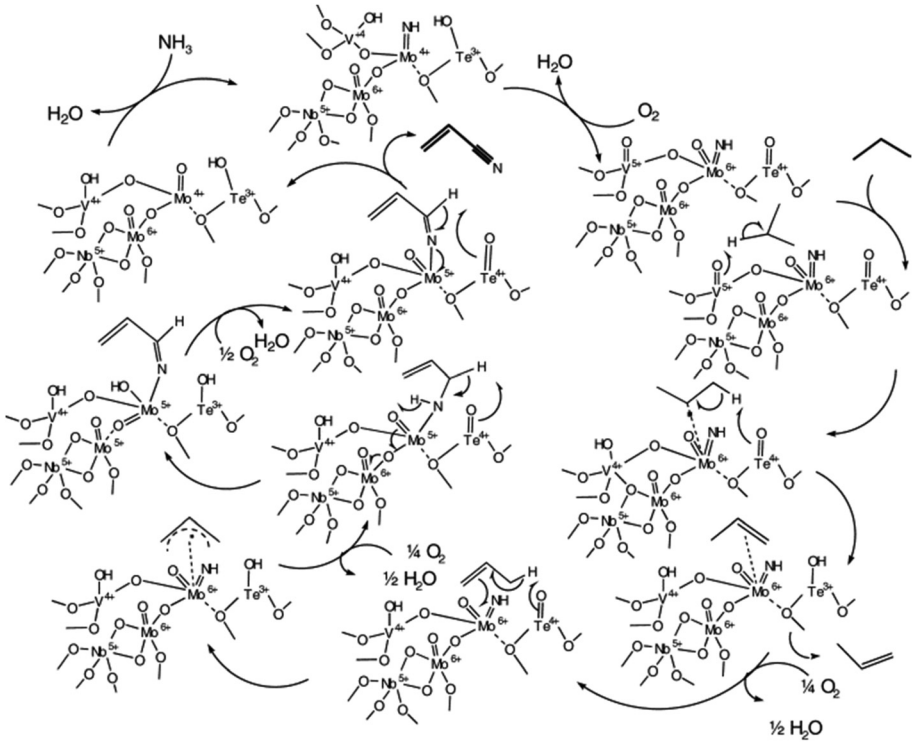

Fig. 6 Proposed propane ammoxidation mechanism over the MoVTeNb mixed oxides catalyst. Reproduced with permission.[69] Copyright 2004, Elsevier B.V.

dation over the M1 phase of the MoVTeNb catalyst was proposed, as shown in Fig. 6.[69]

3.2 Recent 5-years studies on ammoxidation of C_3 hydrocarbons

3.2.1 Propylene ammoxidation. The mechanisms and reaction sequences of propylene ammoxidation have been investigated by using the (010) phase of $Bi_2Mo_3O_{12}$ (see Fig. 7), in which Mo=O sites are perturbed by Bi.[45] The initial hydrogen abstraction from the methyl group of propylene occurred at Bi-perturbed Mo=O sites (site A), and was found to be rate-limiting. Bi^{3+} was proposed to improve propylene adsorption near the Mo=O site and to stabilize surface Mo–OH.[41] An allyl species was formed as an allyl alkoxide and a hydroxyl. The alkoxide species could undergo either the abstraction of its α-hydrogen to form acrolein, or react with adsorbed ammonia on the adjacent Bi^{3+} site to generate allylamine. The formed allylamine has also been evidenced to be an intermediate for AN formation. The allylamine could undergo dehydrogenation of four hydrogens to form AN, or react with an additional adsorbed ammonia to produce diamine species. The diamine has a weak C–C bond that can further be cleaved to form ACN and HCN. Moreover, Mo^{6+} was observed to be reduced to Mo^{4+} during the first hydrogen abstraction step, while Bi^{3+} was not reduced.[41] Under a steady-state condition, Mo remained fully oxidized at Mo^{6+}, indicating that the oxidation of Mo^{4+} to Mo^{6+} is much faster than the reduction of Mo^{6+} to Mo^{4+}. The rapid re-oxidation step of Mo^{4+} to Mo^{6+} was suggested to propel the ammoxidation of propylene.

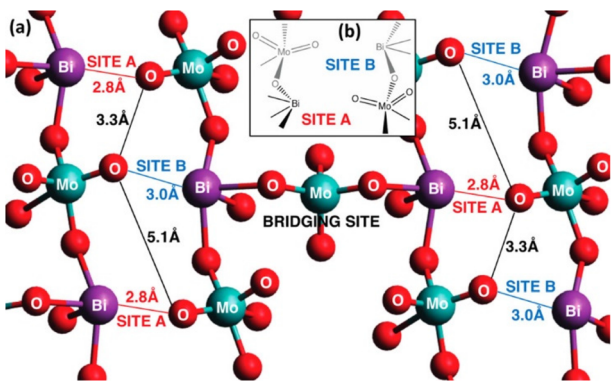

Fig. 7 (a) Top-down view of the optimized (010) surface of $Bi_2Mo_3O_{12}$. All red balls represent oxygen atoms, but only those marked with an "O" are at the surface. (b) Simplified representation of the same surface. Reproduced with permission.[45] Copyright 2016, American Chemical Society.

3.2.2 Propane ammoxidation. Alumina-supported Mo–V mixed oxide in the presence of phosphorus (P) was investigated in propane ammoxidation.[70] The correlation of the P content and AN yield showed a volcano-curve trend with a maximal AN yield at 0.6 wt% P. The authors claimed that phosphorus could weaken an interaction between the support and Mo, inducing a formation of polymeric Mo oxide species.

 This journal is © The Royal Society of Chemistry 2023

Published on 22 February 2023. Downloaded by Yunnan University on 8/24/2025 1:45:34 PM.

Bi was introduced into the orthorhombic Mo_3VO_x (MoVO) using ethyl ammonium cation ($EtNH_3^+$) as a structure-directing agent through hydrothermal synthesis.[71] Bi and $EtNH_3^+$ were located in the hexagonal and heptagonal cavities of MoVO, respectively. With proper thermal treatment, $EtNH_3^+$ could be burnt off, yielding regular heptagonal channels. Compared to the pristine MoVO, the Bi-induced catalyst exhibited a higher propane conversion and a higher AN selectivity due to the space confinement of its heptagonal channels.

MoVTeNb-mixed oxide catalyst was investigated in propane ammoxidation using a microchannel reactor (0.5 × 12.7 × 80 mm).[72] Conventionally, propane ammoxidation was conducted in a packed-bed reactor with a narrow operating temperature window (T = 440–450 °C) to suppress CO_x formation. Moreover, the non-isothermal operation is inevitable due to the exothermic nature of ammoxidation. Thus, a high-temperature difference (~40 °C) could occur in a conventional packed-bed reactor, resulting in the promotion of CO_x. Using a microchannel reactor is a good strategy to address the thermal gradient problem: a negligible temperature gradient (~0.5 °C) was observed in a microchannel reactor. The advantage of using a microchannel reactor is due to its larger surface area-to-volume ratio, facilitating heat transfer with a limited extent of heat accumulation. This allows the propane ammoxidation to be operated under harsher conditions in a microchannel reactor with restrained CO_x selectivity and good stability.

3.3 Synthesis of ACN

3.3.1 Ammodehydrogenation of ethylene. Producing ACN from C_3 hydrocarbons (a C_3-to-C_2 route) indicates that an endothermic C–C cleavage step is needed. Synthesizing ACN from C_2 hydrocarbons (a C_2-to-C_2 route) shall circumvent this energy-demanding step. Non-oxidative production of ACN by using 10% MoO_3-loaded Al_2O_3 was reported at approximately 525 °C with a 1.2 s residence time.[47] A 2-to-1 molar ratio of NH_3-to-hydrocarbon was used as the feed. Among the tested feedstocks (C_2–C_5 hydrocarbons), the highest ACN yield was obtained by using ethylene. This underlined the potential of ACN production from C_2 hydrocarbons.

Takahashi *et al.* reported Al_2O_3 and zeolite-Y (HY) supported Zn^{2+} and Cd^{2+} in the ammodehydrogenation of ethylene.[73,74] The reaction was carried out at 400 °C using a mixture of ethylene (20%), ammonia (20%), and helium (60%). They found that the reactivity of Zn^{2+} and Cd^{2+} loaded on HY is superior to those on Al_2O_3. The ACN formation rate was increased with increasing metal loading. In addition, a small amount of ethylamine was produced, presumably catalyzed by the acid site.[75] They hypothesized that the possible route for ACN formation proceeded *via* ethylamine dehydrogenation. However, by studying the reaction of ethylamine over Zn/Y and Cd/Y catalysts, trace amount of ACN was observed while most ethylamine was decomposed to ethylene and ammonia. The induction period of ACN production from ethylamine was also found, suggesting that ethylamine does not directly convert to ACN. The authors claimed that ACN is produced by the reaction of ethylene and ammonia.

Peeters *et al.* studied the effect of pretreatment procedures (reduction and oxidation) of an Al_2O_3-supported Mo catalyst on ACN production from ethylene in an oxygen-free system.[43,76,77] Dissociative adsorption of NH_3 was a key step for N-insertion in ACN formation from ethylene. =NH species was proposed to be the N-insertion site. Moreover, ACN could only be formed when ethylene was reacted with an ammonia pre-adsorbed catalyst.

Three reaction states were observed for the on-stream tests, including (i) semi-steady state where ACN productivity is constant while others are varied, (ii) transition state where both conversion and productivity fluctuate, and (iii) steady state where both conversion and productivity remain unchanged, illustrated in Fig. 8. In the semi-steady state, a structure-sensi-

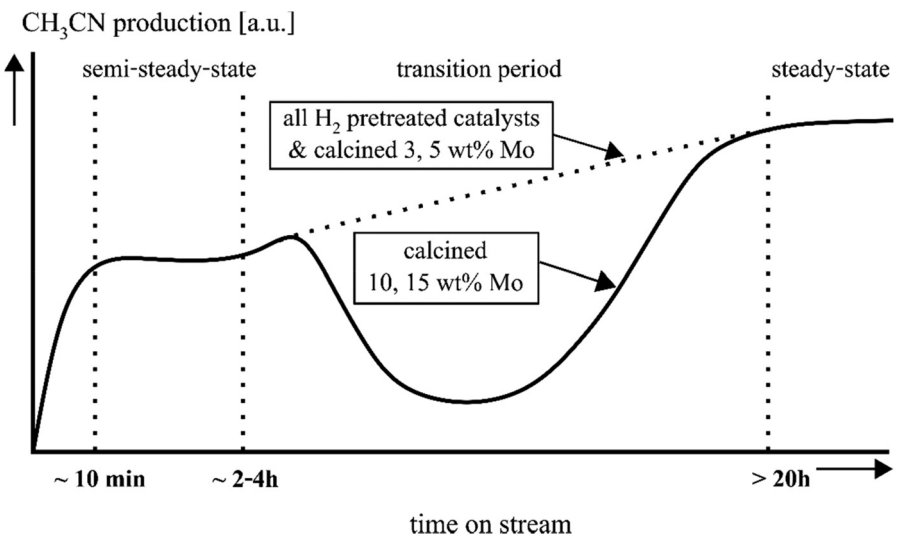

Fig. 8 The TOS profile of ACN formation over the Mo/Al_2O_3 catalyst. Reproduced with permission.[43] Copyright 1998, Academic Press.

Published on 22 February 2023. Downloaded by Yunnan University on 8/24/2025 1:45:34 PM.

tive correlation was revealed. The reduced catalyst (MoO_2-like structure with coexisting Mo^{6+} and Mo^{4+}) exhibited a higher ethylene conversion but a lower ACN selectivity, accompanied by ethane and hydrogen as the byproducts. In contrast, the oxidized catalyst ($Al(MoO_4)_3$ with Mo^{6+} was highly dispersed on the Al_2O_3 surface) had an increasing trend of ethylene conversion and ACN selectivity, in which water and CO_x were byproducts.

During the transition state, all reduced catalysts and oxidized catalysts with less than 5 wt% Mo loading showed gradual increases in ethylene conversion and ACN productivity, then reached a plateau. Oxidized catalysts with 10 and 15 wt% Mo loading exhibited an increase in ethylene conversion, but a sharp decrease in ACN productivity. The authors claimed that at a high Mo loading, the concentration of mobile oxygen can be improved. By contrast, the catalyst at its reduced state and containing a low Mo loading shall possess a small amount of mobile oxygen. Therefore, the ACN depletion was influenced by the concentration of mobile oxygen. During a low ACN production period, the conversion of ethylene and ammonia reached almost 100%. The authors stated that the Mo^{6+} species is not very active toward ethylene conversion, whereas Mo cations with mixed hexa- and tetra-valent states are very active toward side reactions for methane, ethane, CO, hydrogen, and nitrogen formation, resulting in a high ethylene conversion but a low ACN productivity. A reduction of Mo^{6+} to Mo^{4+} was also observed, confirming the removal of mobile oxygen. The side reactions ceased when mobile oxygen was depleted, leading to an increase in ACN productivity. That is, the complete removal of surface mobile oxygen allows the side reactions to be inhibited. The authors proposed that there could be two mechanisms involved, including (i) an ammoxidation mechanism, where mobile oxygen of the catalyst was consumed, and (ii) an ammonolysis mechanism without the consumption of mobile oxygen. The oxidized catalyst proceeded *via* the ammoxidation mechanism since a sharp decrease in ACN production together with mobile oxygen consumption (Mo reduction) was observed.

Under steady-state operation, Mo was in a reduced form (MoO_2-like) regardless of the pretreatments. No oxygen-containing product was observed, and steady on-stream production was obtained. This indicated that the catalyst structure was intact in ammonolysis. Furthermore, the reaction route could be mediated from ammoxidation to ammonolysis when the mobile oxygen of the oxidized catalyst was depleted. Accordingly, it can be stated that Mo ions with a low valence are favored for ammonolysis, while those with a high valence are prone to ammoxidation.

3.3.2 Ammoxidation of ethylene. Ayari *et al.* studied Cr/HZSM-5 for the ammoxidation of ethylene.[78] The authors claimed that Cr cations with a higher oxidation state (*e.g.*, Cr^{6+}) were more active and selective in ammoxidation than its counterpart with a lower state (*e.g.*, Cr^{3+}). A set of chromium precursors including acetate (Cr-A), chloride (Cr-Cl), nitrate (Cr-N), and ammonium dichromate (Cr-D) were used for the solid-state mixing with HZSM-5. Ethylene ammoxidation was performed by using a mixture of O_2 (10%), ethylene (10%), and ammonia (10%) in a He stream at 400 °C, 450 °C, and 500 °C. Among the tested catalysts, Cr-Cl showed the highest activity (26% conversion) and ACN selectivity (95%) at 500 °C. The surface of all catalysts consisted of both Cr^{6+} and Cr^{3+}, in which the ratio of Cr^{6+}/Cr^{3+} was arranged in descending order: Cr-A (1.3) > Cr-Cl (1.1) > Cr-D (0.6) > Cr-N (0.4). Moreover, it was found that Cr-Cl had the highest reducibility. A high Cr^{6+} concentration and strong reducibility were correlated with the activity of ethylene ammoxidation.

The influence of the parent zeolite structure, including MFI (ZSM-5), BEA (beta), MOR (Mor), and FAU (USY and Y), on supported Cr catalysts was investigated for ethylene ammoxidation.[79] The authors found that (poly)chromate species, oxocations, and small Cr_2O_3 clusters are key to ethylene ammoxidation. Moreover, agglomerated Cr_2O_3 could dampen the activity, implying the presence of the particle size effect. Among the selected zeolite supports, immobilizing Cr on ZSM-5 exhibited the highest activity.

ZSM-5-supported Mo, V, and Mo–V oxides catalysts were explored in ethylene ammoxidation.[80,81] Similar to Cr/ZSM-5, monomeric, dimeric, and/or polymeric species were dispersed in the exchangeable sites or external surfaces of the parent ZSM-5 in which the particles were smaller than 4 nm. Over Mo/ZSM-5, the $Al_2(MoO_4)_3$ nano-crystallites were formed. The authors stated that the formation of $Al_2(MoO_4)_3$ could suppress catalytic performance. Substituting Mo with V (1 : 1 by weight) had a synergistic effect on ethylene ammoxidation, achieving 15% conversion and 97% ACN selectivity at 500 °C.[81] It was found that Mo–V/ZSM-5 had a better reversibility in H_2/O_2 redox cycles, and could stabilize the active phase.

3.3.3 ACN synthesis from ethane. Nb-based mixed oxides catalysts were studied for ethane ammoxidation.[42,82,83] Catani and Centi discovered that Al_2O_3-supported Nb–Sb mixed oxides were active for ethane ammoxidation, obtaining approximately 25% ethane conversion and 50% ACN selectivity at 500 °C.[42] Ethylene was observed at low conversions and progressively decreased at higher conversions. They suggested that the formed ethylene is an intermediate for ACN formation.

In line with this view, V–Mo–Nb oxides catalysts, in which the Mo_5O_{14}-like structure was suggested to be active sites, also showed the same trend for ethane ammoxidation. The ACN selectivity was nearly unaltered, whereas those of the carbon oxides were promoted with increasing conversion.[82] Moreover, at the same ethane conversion level (10%), it was found that a high Nb content in the catalysts can suppress the formation of carbon oxides. They further claimed that Nb is highly selective toward ethane ammoxidation.

Nb-modified NiO catalysts were also promising for ethane ammoxidation since it was efficient for the oxidative dehydrogenation of ethane.[83] Well-defined NiO and Nb_2O_5 structures were not reactive toward ethane ammoxidation. Doping a small amount of Nb to NiO ($Ni_{0.9}Nb_{0.1}$) could enhance both ethane conversion and ACN selectivity (55% ethane conversion and 35% ACN selectivity at 450 °C). However, a further increase

 This journal is © The Royal Society of Chemistry 2023

Published on 22 February 2023. Downloaded by Yunnan University on 8/24/2025 1:45:34 PM.

in Nb content led to the formation of Ni–Nb–O phases, which were dehydrogenation-active. The performance of Ni–Nb–O catalysts was further improved using nanoscale particles.[15,84] A new phase of $NiNb_2O_6$ was observed through catalyst nanocrystallization. The authors claimed that a ratio of $NiNb_2O_6$/NiO close to 0.5 is necessary to obtain desired performances (25% ethane conversion and 80% ACN selectivity at 425 °C).

The reaction mechanism of ethane ammoxidation over Ni–Nb–O was proposed to occur on the Nb-disturbed NiO surface.[85] The methyl group of ethane was activated over the disturbed-Ni site, forming the ethyl group on the Ni surface and –OH group on the adjacent oxygen (Fig. 9).[86] Ethylene was formed by β-H cleavage to another adjacent bare oxygen, producing another –OH species. The catalyst was then regenerated by dehydration using gaseous oxygen. However, the sequence of the N-insertion of ethylene to ACN is still unclear, which is proposed to occur either by the pre-adsorbed ammonia or in the gas phase.

The Armor group studied metal/zeolite catalysts for ethane ammoxidation.[43,87] The reaction was conducted at 450 °C using a mixture of ethane (5%), ammonia (10%), and oxygen (6.5%) balanced with helium. Various transition metals such as Co, Cu, Ni, Fe, Mn, Pd, Ag, Rh, and Pt loaded on ZSM-5 were screened. ACN could only be produced by non-noble metals, excluding Cu. Among the tested catalysts, Co exhibited the best performance (38% conversion and 49% ACN selectivity). Noble metals were highly active in ethane combustion. Accordingly, reducible metals with oxophilicity are proposed to be favored for ethane ammoxidation. Zeolite topologies were also investigated. It was found that ZSM-5 and BEA were the most appropriate supports for immobilizing Co ions. Co ions were found to be located at the junction of the straight and sinusoidal channels in ZSM-5, and to be anchored in the open channels of BEA.[88] These sites are deemed to be important in ethane ammoxidation.

The reaction pathway of ammoxidation of ethane and ethylene was studied by using Co/ZSM-5.[44] The authors

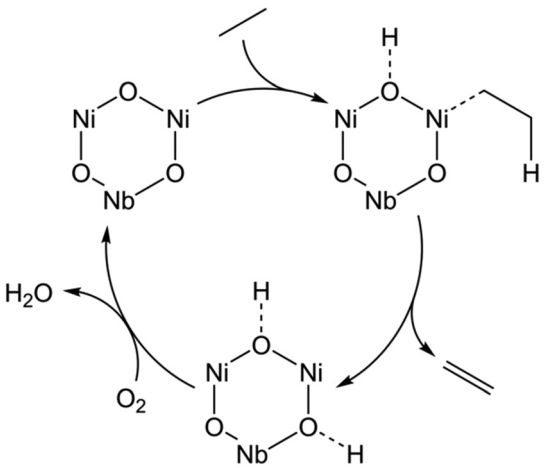

Fig. 9 Schematic diagram of the oxidative dehydrogenation of ethane to ethylene over Nb–Ni–O oxide.[85,86]

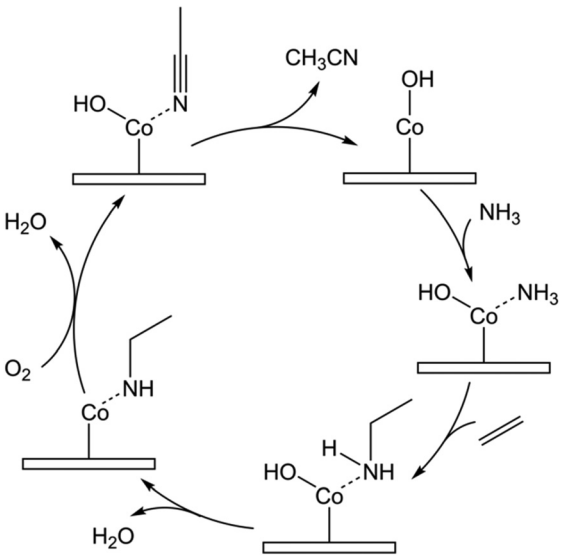

Fig. 10 Ethane ammoxidation mechanism over the Co/ZSM-5 catalyst.[44]

claimed that the strong NH_3 adsorption on hydroxylated Co^{2+} (Co–OH) was the key step to initiate ammoxidation (Fig. 10). Ethylene (formed from ethane oxidative dehydrogenation) was then reacted with pre-adsorbed NH_3, generating ethylamine ($C_2H_5NH_2$) on Co^{2+}. The formation of ethylamine was evidenced by the temperature-programmed reaction of ammonia-adsorbed Co/ZSM-5 by using an ethylene and O_2 mixture as the feed. The adsorbed ethylamine was then dehydrogenated by coupling with the adjacent OH, forming water and the intermediate, *i.e.*, C_2H_5NH. C_2H_5NH was sequentially reacted with O_2 to produce ACN and an OH group adsorbed on Co^{2+}. Kinetic studies on Co/ZSM-5 revealed that the ACN formation rate was first order in ammonia and was 0.8 order in oxygen.[87] This confirms that the adsorption of ammonia is important and the reaction of a surface intermediate with gaseous O_2 is possible, analogous to the Eley–Rideal mechanism.

3.4 Recent 5-years studies on ACN synthesis from C_2 hydrocarbons

Ammoxidation of ethane produces valuable products, including ethylene and ACN, resulting in a recent boom in ethane ammoxidation research.

The conventional Co/BEA catalyst was able to be improved by using the solid-state ion exchange method (SSIE).[89] The authors reported that using either conventional solid-state ion exchange or impregnation with $[Co(OH_2)_6]^{2+}$ complex would lead to the formation of ammoxidation-inactive Co_3O_4 species. The improved impregnation method was performed by using the $[Co(NH_3)_6]^{2+}$ complex, forming nitride (Co_4N) as the active phase. The ammoxidation activity can be 2-fold higher than those of the conventional Co/BEA catalysts (from 24% to 48% ethane conversion and 90% ACN selectivity at 450 °C). Moreover, the exchange of $[Co(OH_2)_6]^{2+}$ by $[Co(NH_3)_6]^{2+}$

Published on 22 February 2023. Downloaded by Yunnan University on 8/24/2025 1:45:34 PM.

complex could inhibit the formation of Co_3O_4 species due to the confinement effect of the BEA zeolite topology.

Liu *et al.* supported the claim that enhancing Co^{2+} dispersion in the zeolite was beneficial for ammoxidation, while the agglomerated Co_3O_4 species were active toward combustion.[90] They also suggested that excessive Brønsted acid acted as a receptacle for NH_3, which enhanced ACN formation and suppressed combustion. A transient analysis also discovered that NH_3 mediated the initial oxidative dehydrogenation of ethane. The back-transient analysis showed the same decays of NH_3 and CO_2, suggesting CO_2 formation was inhibited when NH_3 is present.

Alternatively, the Sn/HZSM-5 catalyst has been discovered for ethane ammoxidation.[91] At a similar level of ethane conversion (*e.g.*, 10%), the Sn catalyst exhibited a higher ACN selectivity than the Co catalyst (80% and 60%, respectively). The Sn^{4+} species was suggested to be active for ACN production, whereas SnO_x would reduce ACN and increase CO_2 yields. The transient kinetics analysis showed that the reaction pathway of ethane ammoxidation over the Sn catalyst was similar to that of the Co catalyst. At the outset of ethane ammoxidation, ethylene was the major product over Sn/HZSM-5, whereas CO_2 dominated by using Co/HZSM-5. The authors thereby differentiate the Sn-directed and Co-directed ethane ammoxidation routes.

Non-oxidative ammodehydrogenation of ethane was studied over the Pt/HZSM-5 catalyst at 350–650 °C using an ethane/NH_3 ratio of 1.[92] The authors found that both metal sites and Brønsted acid site are necessary for dehydrogenation and N-insertion. At 350 °C, 99% ACN selectivity was obtained. However, the conversion of ethane was only 1%. A further increase in the reaction temperature could enhance the conversion with a compensate ACN selectivity. The tandem reaction mechanism of dehydrogenation (ethane to ethylene), amination (ethylene to ethylamine), and dehydrogenation (ethylamine to ACN) was proposed, in which the dehydrogenation could be catalyzed by metallic Pt sites; amination, Brønsted acid sites.

Several promoters were investigated to enhance ethane ammodehydrogenation activity of Pt/HZSM-5.[38] Only Co showed desirable results by modifying both metal and acid functionalities. Co-promoted Pt/HZSM-5 exhibited 20% initial ethane conversion with 65% ACN selectivity, while non-promoted Pt/HZSM-5 showed 15% conversion and 63% selectivity at 500 °C. Additionally, the authors conducted ethylene ammodehydrogenation over Re/HZSM-5. Besides ACN, byproducts including ethane, C_3^+, and BTX were generated. These byproducts were produced over the Brønsted acid site *via* the oligomerization of ethylene. Therefore, the ethylene content in the reaction stream should be properly controlled. The composition of the metal and acid sites was also suggested to be critical for both ethane and ethylene ammodehydrogenation.

The ammoxidation of C_{2-3} hydrocarbons is summarized in Table 1. Mo-based catalysts seem to be the most promising candidates for direct propane ammoxidation to AN. In the case of ethane ammoxidation to ACN, most research focused on metal-loaded zeolite, particularly ZSM-5 and BEA. Co-based catalysts seemed to show higher activities among reported catalysts. However, bare Co^{2+} ions were unstable. Improving the stability of immobilized metal ions in zeolites under reaction conditions would facilitate the practice of ethane conversion. Ammodehydrogenation can be facilitated by noble metal modified zeolite, particularly ZSM-5. The cooperation of metal for dehydrogenation and the Brønsted acid for amination shall enhance both ethane conversion and ACN productivity.

3.5 Methane conversion to ACN

Synthesis of ACN from methane can be dated back to the 1960s.[93] Hydrogen cyanide (HCN) was used as a co-feed in the conversion of methane to ACN process. This noncatalytic

Table 1 Summary of the ammoxidation of C_3 and C_2 hydrocarbons

Reaction	Catalyst	Feed/NH_3/O_2 ratio	Reaction temp. (°C)	Conversion (%)	Sel. (%)	Ref.
Propylene ammoxidation	BiPMo	1/1.1/13.1 (air)	470	95	AN, 68	39
Propane ammoxidation	Mo–Sb	1/0.7/4.8 (air)	550	29	AN, 15	57
	Mo–Ce (CH_3Br additive)	1/1.2/12 (air)	500	98	AN, 65	58
	Bi–V–Mo	5/1/2	470	12	AN, 61	59–61
	Sb–V	1/2/2	500	67	AN, 60	62–64
	MoVTeNb	1/1.2/3	420	76	AN, 66	68
	Mo–V–P	1/1.5/3	430	50	AN, 34	70
	Mo–V–Bi	1/1.3/3	440	60	AN, 20	71
Ethylene ammoxidation	Cr/HZSM-5	1/1/1	500	26	ACN, 95	78
	Mo–V/ZSM-5	1/1/1	500	15	ACN, 97	81
Ethane ammoxidation	Nb–Sb/Al_2O_3	1/0.6/1.6	500	25	ACN, 50	42
	V–Mo–Nb	5/6/6	400	15	ACN, 25	82 and 83
	Ni–Nb–O	1/0.9/2.6	450	55	ACN, 35	83
	Ni–Nb–O	1/0.9/2.6	425	25	ACN, 80	84
	Co/ZSM-5	1/2/1.3	450	38	ACN, 49	87
	Co/BEA	1/1/1	450	48	ACN, 90	89
	Sn/HZSM-5	1/1/0.6	550	10	ACN, 80	91
Ethane ammodehydrogenation	Pt/HZSM-5	1/1/0	500	15	ACN, 63	92
	CoPt/HZSM-5	1/1/0	500	20	ACN, 65	38
Ethylene ammodehydrogenation	Re/HZSM-5	1/1/0	500	20	ACN, 80	38

 This journal is © The Royal Society of Chemistry 2023

Published on 22 February 2023. Downloaded by Yunnan University on 8/24/2025 1:45:34 PM.

process requires harsh conditions (T = 850–950 °C and a low space velocity of 150–500 h^{-1}). Regretfully, ACN can be decomposed at temperatures higher than 800 °C, in which a low ACN yield was obtained.[94] The unsatisfactory results usher in the development of heterogeneous catalysis in ACN generation from methane.

To produce ACN from methane, C–H activation and cyanation are important. Venu *et al.* reported that the cyanation of the C–H bond can be promoted by bases of hydroxyapatite (HAP)-supported Cu catalysts.[95] Although the HAP contained basicity (173 μmol g^{-1}), there is no activity observed over the HAP support. This indicates that the basic sites of the parent HAP play a minor role in cyanation. They thereby claimed that the O^{2-} species possessed the basicity on the Cu surface, and were responsible for the cyanation of the C–H bond of methane. Metal nitrides are known to be Lewis bases[96] and GaN has been recently applied for methane conversion to hydrocarbons.[97,98] Thus, the C–H activation can be catalyzed over GaN. Accordingly, GaN is a promising basic catalyst for C–H bond activation and cyanation.

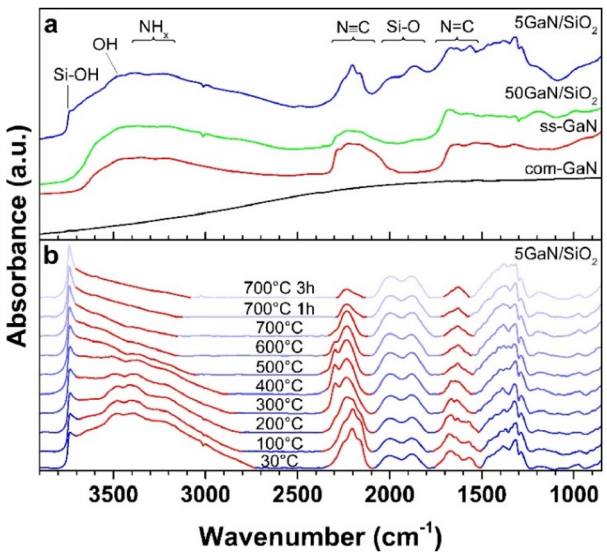

Fig. 11 FTIR spectra of (a) fresh GaN catalysts and (b) a temperature-resolved *in situ* analysis of 5GaN/SiO_2 from 30 to 700 °C. Reproduced with permission.[100] Copyright 2021, Elsevier B.V.

GaN can be synthesized by two major methods, *i.e.*, ammonia nitridation of Ga_2O_3 and co-pyrolysis of gallium nitrate with a N-containing precursor. The former usually treats Ga_2O_3 in a high concentration of gaseous ammonia (99%) at 700 °C and up for a long period. The latter pyrolyzed mixed Ga (*e.g.*, gallium nitrate) and N precursors (*e.g.*, melamine) in an oxygen-free system at approximately 800 °C for 1 h, and subsequently calcined the sample at 550 °C to "clean" the surface by removing residue carbon.[99] It should be noted that C–H bond cyanation needs the presence of the CN species. Accordingly, the co-pyrolysis of gallium nitrate with melamine was adopted to synthesize GaN without the calcination step for methane conversion to ACN.

Our group recently reported the solid-state-pyrolysis-made GaN (ss-GaN) as a catalyst for methane conversion to ACN.[100] The commercially available GaN (com-GaN) was used as a reference to compare the ACN production rate. Amorphous SiO_2 was also selected as a support to disperse GaN crystals (*e.g.*, 5 and 50 wt% loadings, 5GaN/SiO_2 and 50GaN/SiO_2, respectively). The reaction was carried out at 700 °C using a horizontal fixed-bed flow reactor. Surprisingly, cyanide products including HCN and ACN can be produced from methane over the ss-GaN catalyst, whereas com-GaN shows a negligible cyanide formation rate. Moreover, the ACN production rate per gram of Ga is increased with decreasing Ga loading. The low GaN crystallites and the high dispersion of ss-GaN were thereby proposed to be vital.

An explanation of the varying activities between ss-GaN and com-GaN can be made by referring to the different surface natures. The XPS spectra at N 1s of fresh ss-GaN catalysts contained N≡C and N=C species (CN species) together with N–H and N–Ga groups, whereas only N–H and N–Ga responses were observed on the com-GaN catalyst. The surface CN species were claimed to participate in the formation of ACN from methane since the responses of the CN species decreased after the reaction. Further analysis by *in situ* FTIR (Fig. 11) showed that the vibrational peaks of the CN species can be observed over the ss-GaN catalysts, and gradually declined in the CH_4 stream in a temperature-programmed reaction test of 5GaN/SiO_2. A plausible mechanism was proposed by methylation of surface CN species, as shown in Fig. 12. The proposed mechanism was validated by H_2 co-feeding experiment, showing a decreased ACN yield by compensating with an increased HCN yield through the suppression of methylation by hydrogen.

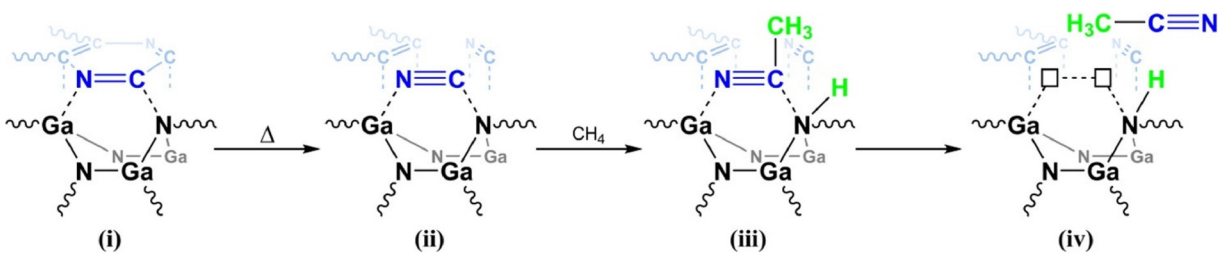

Fig. 12 Proposed mechanism of ACN production over solid-state-made GaN catalysts. Reproduced with permission.[100] Copyright 2021, Elsevier B.V.

Published on 22 February 2023. Downloaded by Yunnan University on 8/24/2025 1:45:34 PM.

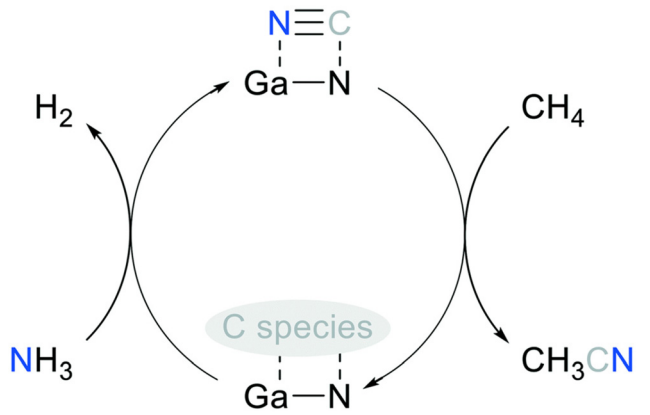

Fig. 13 Proposed catalytic cycle of methane conversion to ACN over solid-state-made GaN catalysts. Reproduced with permission.[101] Copyright 2022, the Royal Society of Chemistry.

This underlined that the CN species were the key intermediate in ACN formation.

The influence of the N-source and the structure–activity correlation was also investigated.[101] GaN crystallites were tailored by using different N-sources, including melamine, melem, and g-C_3N_4, and different ratios of N-precursor to Ga-precursor. Finely dispersed GaN can be obtained when g-C_3N_4 was utilized. Moreover, GaN crystallite size is reduced with the increase of the N/Ga ratio. An accumulated ACN productivity is enhanced by shrinking GaN crystallite size and by improving the sp^3-N/sp^2-N ratio. However, the formation of ACN still consumes surface CN species, resulting in catalyst deactivation. N-depleted GaN catalyst could be rejuvenated through a direct nitridation process to recover ACN productivity partially, likely due to the transformation of surface carbonaceous species to CN species after nitridation. The catalytic cycle was proposed (Fig. 13).

4. Summary, challenges, and outlook

AN synthesis from propylene has been commercialized for over 60 years. Various studies were conducted according to the catalyst design for further development of this process. Still, the commercial catalyst (50% SiO_2-supported $Bi_9PMo_{12}O_{52}$) is unbeatable. However, the drained oil reservoirs and advanced shale gas harvesting technology shall usher in the substitution of propylene by using C_1–C_3 alkanes as the feedstocks. Accordingly, studies on direct propane ammoxidation or tandem propane dehydro-ammoxidation processes would be promising for the next generation of AN production. In addition, the synthesis of AN from the biomass-derived compound, glycerol, would be attractive.[4,102,103]

The in-depth mechanism and surface intermediates of propane ammoxidation remain to be clarified. Presumably, the formed intermediates have promptly undergone the succeeding steps of the reaction. In this case, a propane pulsing technique (*e.g.*, steady state isotopic transient kinetic analysis, SSITKA) and theoretical calculation (*e.g.*, density functional theory) shall reveal the unnoticeable surface intermediates, and therefore provide useful information for a rational catalyst design. MoVTeNb mixed oxides catalyst seems to be the most promising catalyst due to its multifunctionality. The higher percentage of the orthorhombic (M1) phase shows a better AN yield. However, the yield is almost level off at % M1 phase higher than 50 (see Fig. 5). It was stated that to achieve the highest AN selectivity, propylene produced from the M1 phase must migrate to the M2 phase to avoid overoxidation. Moreover, smaller catalyst grains could enhance AN selectivity, presumably due to the shorter migration time. Therefore, precisely controlling the grain size and space between these two phases (M1 and M2) is recommended.

Direct ACN production, either from ethylene or ethane ammoxidation, is not yet practiced at a commercial level. Again, the ammoxidation of ethane would be feasible in the future because of the growing shale gas industry. The aforementioned studies revealed that reducible oxophilic metals are suitable for this reaction. Moreover, the Sn/HZSM-5 catalyst showed a better ACN selectivity, while Co/HZSM-5 exhibited a high ethane conversion. Using the same approach as propylene ammoxidation, a multi-metal oxides catalyst would be promising in terms of enhancing both ethane conversion and selectivity. Moreover, a bare metal ion (*i.e.*, Co^{2+}) located at exchangeable sites of zeolite is active for ethane ammoxidation. Still, its stability remains to be improved. Gallium is known to be an exchangeable cation within zeolite cavities ($[Ga(OH)_2]^+$, $[GaO]^+$, $[GaH_2]^+$, or Ga^+),[104,105] and is active for light alkane dehydrogenation. Accordingly, Ga/HZSM-5 would be worthy to investigate in ethane ammoxidation.

Noble metals loaded on ZSM-5 shows a promising application in ammodehydrogenation of ethane to ACN. The major challenge is the thermodynamics limitation of ethylene oligomerization, hindering the high ethane conversion operation. Tailoring the metal–acid (both Brønsted and Lewis acid) functionalities could be the key for further catalyst design.

Synthesis of ACN from methane has been done using solid-state-pyrolysis-made GaN catalysts. However, ACN was produced by the carbon residue on the catalyst surface. Taking ammonia synthesis from metal nitrides as a probe reaction,[96] it proceeds by a reaction of gaseous hydrogen with lattice nitrogen of the nitride catalyst. Hence, the reaction of methane with lattice nitrogen of residue-free GaN-based catalyst would be promising. In addition, ACN was previously produced from methane by the noncatalytic addition of HCN. The operation conditions were harsh, in which ACN could be decomposed. Therefore, innovating the catalytic system of methane conversion to ACN with HCN as the co-reactant would have the potential to utilize toxic HCN.

Although the price of AN and ACN is higher than that of hydrocarbons, the value stated in this work does not include the cost of production and the environmental sustainability. Therefore, it is also crucial to analyze those factors for further industrial practice. Life cycle assessment (LCA) is an attracting

 This journal is © The Royal Society of Chemistry 2023

Published on 22 February 2023. Downloaded by Yunnan University on 8/24/2025 1:45:34 PM.

tool for catalysis research.[106] It can provide the environmental impact of different chemical processes. For example, the existing propylene ammoxidation process (Sohio) was compared to an alternative propane ammoxidation route in terms of environmental sustainability.[107] It was found that the selected route has more impact regarding fossil fuel depletion and climate change because of its higher consumption of the propane feed. However, only a single reactor was applied for LCA analysis. It could also be promising for further analysis by using an integrated dehydrogenation–ammoxidation process. Moreover, other processes including ethane, ethylene, ethanol, and methane conversion to ACN should be studied to explore the possibility of each reaction for industrial practice.

Conflicts of interest

The authors declare that they have no competing financial interests.

Acknowledgements

This work was supported by the National Science and Technology Council (projects 109-2628-E-006-011-MY3, 110-2221-E-006-165-MY3, 110-2923-E-006-005-MY3, and 110-2927-I-006-506).

References

1 E. Rojas, J. J. Delgado, M. O. Guerrero-Pérez and M. A. Bañares, *Catal. Sci. Technol.*, 2013, **3**, 3173–3182.
2 J. F. Brazdil, *Ullmann's Encyclopedia of Industrial Chemistry*, 2012. DOI: **10.1002/14356007.a01_177.pub3**.
3 J. M. Thomas and W. J. Thomas, *Principles and practice of heterogeneous catalysis*, John Wiley & Sons, 2014.
4 R. K. Grasselli and F. Trifirò, *Top. Catal.*, 2016, **59**, 1651–1658.
5 E. M. Karp, T. R. Eaton, V. Sànchez i Nogué, V. Vorotnikov, M. J. Biddy, E. C. D. Tan, D. G. Brandner, R. M. Cywar, R. Liu, L. P. Manker, W. E. Michener, M. Gilhespy, Z. Skoufa, M. J. Watson, O. S. Fruchey, D. R. Vardon, R. T. Gill, A. D. Bratis and G. T. Beckham, *Science*, 2017, **358**, 1307–1310.
6 A. C. C. P. Department, *The Chemistry of Acrylonitrile*, Synthetic Organic Chemicals Department, American Cyanamid Company, 1951.
7 M. A. Dalin, I. K. Kolchin and B. R. SerebriĺĄakov, *Acrylonitrile*, Technomic Publication, 1971.
8 C. E. Habermann and B. A. Tefertiller, *US Pat.*, 3631104, 1971.
9 W. A. Barber and J. A. Fetchin, *US Pat.*, 4048226, 1977.
10 K. Matsuda and W. A. Barber, *US Pat.*, 4086275, 1978.
11 J. A. Fetchin and K. H. Tsu, *US Pat.*, 4178310, 1979.
12 M. M. Baizer, C. R. Campbell, R. H. Fariss and R. Johnson, *US Pat.*, 3193480, 1965.
13 J. W. Badham, *US Pat.*, 3529011, 1970.
14 I. F. McConvey, D. Woods, M. Lewis, Q. Gan and P. Nancarrow, *Org. Process Res. Dev.*, 2012, **16**, 612–624.
15 E. Rojas, M. O. Guerrero-Pérez and M. A. Bañares, *Catal. Lett.*, 2013, **143**, 31–42.
16 X. Yang, S. Wang, G. Li, F. Zhao, Z. Feng, X. Chen, Z. Zhu, Y. Wang and J. Gao, *Ind. Eng. Chem. Res.*, 2020, **59**, 5047–5055.
17 W. Ueda, T. Yokoyama, Y. Moro-Oka and T. Ikawa, *Ind. Eng. Chem. Prod. Res. Dev.*, 1985, **24**, 340–342.
18 E. L. Carpenter, *US Pat.*, 2690452, 1954.
19 P. H. DeBruin, *US Pat.*, 2729670, 1956.
20 E. G. Hancock, *Propylene and Its Industrial Derivatives*, Wiley, 1973.
21 K. Sennewald, World Petroleum Congress Proceedings, 1959.
22 N. Brown, *US Pat.*, 2554482, 1951.
23 L. R. U. Spence and F. O. Haas, *US Pat.*, 2385552, 1945.
24 D. C. England and G. V. Mock, *US Pat.*, 2736739, 1956.
25 E. B. Huntley, J. M. Kruse and J. W. Way, *US Pat.*, 3184415, 1965.
26 A. Tripodi, D. Ripamonti, R. Martinazzo, F. Folco, T. Tabanelli, F. Cavani and I. Rossetti, *Chem. Eng. Sci.*, 2019, **207**, 862–875.
27 F. Folco, J. Velasquez Ochoa, F. Cavani, L. Ott and M. Janssen, *Catal. Sci. Technol.*, 2017, **7**, 200–212.
28 T. Tabanelli, M. Mari, F. Folco, F. Tanganelli, F. Puzzo, L. Setti and F. Cavani, *Appl. Catal., A*, 2021, **619**, 118139.
29 S. J. Kulkarni, R. R. Rao, M. Subrahmanyam and A. V. R. Rao, *J. Chem. Soc., Chem. Commun.*, 1994, 273, DOI: **10.1039/C39940000273**.
30 A. Tripodi, M. Compagnoni, G. Ramis and I. Rossetti, *Chem. Eng. Res. Des.*, 2017, **127**, 92–102.
31 A. Tripodi, D. Manzini, M. Compagnoni, G. Ramis and I. Rossetti, *J. Ind. Eng. Chem.*, 2018, **59**, 35–49.
32 Y. Wei, Z. Liu, G. Wang, Y. Qi, L. Xu, P. Xie and Y. He, in *Stud. Surf. Sci. Catal*, ed. J. Čejka, N. Žilková and P. Nachtigall, Elsevier, 2005, vol. 158, pp. 1223–1230.
33 S. Zendehboudi and A. Bahadori, in *Shale Oil and Gas Handbook*, ed. S. Zendehboudi and A. Bahadori, Gulf Professional Publishing, 2017, pp. 1–26. DOI: **10.1016/B978-0-12-802100-2.00001-0**.
34 A. Sieminski, US Energy Information Administration, 2015.
35 J. J. Sattler, J. Ruiz-Martinez, E. Santillan-Jimenez and B. M. Weckhuysen, *Chem. Rev.*, 2014, **114**, 10613–10653.
36 Intratec, Commodity Price Benchmarks, **https://www.intratec.us/**.
37 J. E. Mahan, *US Pat.*, 2535082, 1950.
38 G. Chen, S. Fadaeerayeni, L. Fang, E. Sarnello, T. Li, H. Toghiani and Y. Xiang, *Catal. Today*, 2022, DOI: **10.1016/j.cattod.2022.05.016**.
39 F. Veatch, J. L. Callahan, J. D. Idol and E. C. Milberger, *Hydrocarbon Process. Pet. Refin.*, 1962, **41**, 187–190.
40 H. A. Deepa, R. Anusha and P. Asha, *Int. J. Eng. Res. Technol.*, 2016, **4**, 1–6.
41 A. T. Bell, *J. Catal.*, 2022, **408**, 436–452.

Published on 22 February 2023. Downloaded by Yunnan University on 8/24/2025 1:45:34 PM.

42 R. Catani and G. Centi, *J. Chem. Soc., Chem. Commun.*, 1991, 1081–1083, DOI: 10.1039/C39910001081.
43 I. Peeters, A. W. D. van der Gon, M. A. Reijme, P. J. Kooyman, A. M. de Jong, J. van Grondelle, H. H. Brongersma and R. A. van Santen, *J. Catal.*, 1998, **173**, 28–42.
44 Y. Li and J. N. Armor, *J. Catal.*, 1998, **176**, 495–502.
45 R. B. Licht and A. T. Bell, *ACS Catal.*, 2017, **7**, 161–176.
46 L. D. Schmidt, *The engineering of chemical reactions*, Oxford University Press, New York, 1st edn, 1998.
47 W. I. Denton and R. B. Bishop, *Ind. Eng. Chem.*, 1953, **45**, 282–286.
48 W. K. Lewis, E. R. Gilliland and W. A. Reed, *Ind. Eng. Chem.*, 1949, **41**, 1227–1237.
49 J. L. Callahan, R. K. Grasselli, E. C. Milberger and H. A. Strecker, *Ind. Eng. Chem. Prod. Res. Dev.*, 1970, **9**, 134–142.
50 C. R. Adams and T. J. Jennings, *J. Catal.*, 1963, **2**, 63–68.
51 W. M. H. Sachtler, *Recl. Trav. Chim. Pays-Bas*, 1963, **82**, 243–245.
52 C. R. Adams and T. J. Jennings, *J. Catal.*, 1964, **3**, 549–558.
53 C. R. Adams, *Proc. Int. Congr. Catal.*, 1965, **1**, 240–249.
54 W. M. H. Sachtler and N. H. deBoer, *Proc. Int. Congr. Catal.*, 1965, **1**, 252–263.
55 G. Centi, R. K. Grasselli and F. Trifiro, *Catal. Today*, 1992, **13**, 661–666.
56 R. Nilsson, T. Lindblad and A. Anderson, *J. Catal.*, 1994, **148**, 501–513.
57 K. Sargis, *US Pat.*, 3365482, 1968.
58 G. Tullman, *US Pat.*, 3746737, 1973.
59 L. C. Glaeser and J. F. Brazdil, *US Pat.*, 4843055, 1989.
60 L. C. Glaeser, J. F. Brazdil and M. A. Toft, *US Pat.*, 4835125, 1989.
61 L. C. Glaeser, J. F. Brazdil and M. A. Toft, *US Pat.*, 4837191, 1989.
62 A. T. Guttmann, R. K. Grasselli and J. F. Brazdil, *US Pat.*, 4746641, 1988.
63 A. T. Guttmann, R. K. Grasselli and J. F. Brazdil, *US Pat.*, 4788317, 1988.
64 M. A. Toft, J. F. Brazdil and L. C. Glaeser, *US Pat.*, 4784979, 1988.
65 S. Albonetti, G. Blanchard, P. Burattin, T. J. Cassidy, S. Masetti and F. Trifiro, *Catal. Lett.*, 1997, **45**, 119–123.
66 M. O. Guerrero-Pérez, A. J. McCue and J. A. Anderson, *J. Catal.*, 2020, **390**, 72–80.
67 D. Melzer, G. Mestl, K. Wanninger, A. Jentys, M. Sanchez-Sanchez and J. A. Lercher, *Top. Catal.*, 2020, **63**, 1754–1764.
68 R. K. Grasselli, J. D. Burrington, D. J. Buttrey, P. DeSanto, C. G. Lugmair, A. F. Volpe and T. Weingand, *Top. Catal.*, 2003, **23**, 5–22.
69 R. K. Grasselli, *Catal. Today*, 2005, **99**, 23–31.
70 M. Baek, J. K. Lee, H. J. Kang, B. J. Kwon, J. H. Lee and I. K. Song, *Catal. Commun.*, 2017, **92**, 27–30.
71 S. Ishikawa, Y. Goto, Y. Kawahara, S. Inukai, N. Hiyoshi, N. F. Dummer, T. Murayama, A. Yoshida, M. Sadakane and W. Ueda, *Chem. Mater.*, 2017, **29**, 2939–2950.
72 J. Lin, J. Tian, X. Cheng, J. Tan, S. Wan, J. Lin and Y. Wang, *AlChE J.*, 2018, **64**, 4002–4008.
73 N. Takahashi, H. Minoshima and H. Iwadera, *Chem. Lett.*, 1994, **23**, 1323–1324.
74 N. Takahashi, H. Sakagami, N. Okabe, Y. Sekimura, H. Minami, N. Okazaki, T. Matsuda and Y. Imizu, *Appl. Catal., A*, 1997, **164**, 281–289.
75 M. Deeba, M. E. Ford and T. A. Johnson, *J. Chem. Soc., Chem. Commun.*, 1987, 562–563.
76 I. Peeters, *Doctor of Philosophy*, Technische Universiteit Eindhoven, 1996.
77 I. Peeters, J. van Grondelle and R. A. van Santen, *Heterogeneous Hydrocarbon Oxidation*, American Chemical Society, 1996, ch. 23, vol. 638, pp. 319–329.
78 F. Ayari, M. Mhamdi, D. P. Debecker, E. M. Gaigneaux, J. Alvarez-Rodriguez, A. Guerrero-Ruiz, G. Delahay and A. Ghorbel, *J. Mol. Catal. A: Chem.*, 2011, **339**, 8–16.
79 F. Ayari, M. Mhamdi, J. Álvarez-Rodríguez, A. R. Guerrero Ruiz, G. Delahay and A. Ghorbel, *Appl. Catal., A*, 2012, **415–416**, 132–140.
80 B. Rhimi, M. Mhamdi, A. Ghorbel, V. N. Kalevaru, A. Martin, M. Perez-Cadenas and A. Guerrero-Ruiz, *J. Mol. Catal. A: Chem.*, 2016, **416**, 127–139.
81 B. Rhimi, M. Mhamdi, V. N. Kalevaru and A. Martin, *RSC Adv.*, 2016, **6**, 65866–65878.
82 V. M. Bondareva, V. M. Bondareva, T. V. Andrushkevich, T. V. Andrushkevich, G. I. Aleshina, G. I. Aleshina, L. M. Plyasova, L. M. Plyasova, L. S. Dovlitova, L. S. Dovlitova, O. B. Lapina, O. B. Lapina, D. F. Khabibulin, D. F. Khabibulin and A. A. Vlasov, *React. Kinet. Catal. Lett.*, 2006, **87**, 377–386.
83 E. Rojas, M. O. Guerrero-Pérez and M. A. Bañares, *Catal. Commun.*, 2009, **10**, 1555–1557.
84 F. Rubio-Marcos, E. Rojas, R. López-Medina, M. O. Guerrero-Pérez, M. A. Bañares and J. F. Fernandez, *ChemCatChem*, 2011, **3**, 1637–1645.
85 M. O. Guerrero-Pérez, E. Rojas-García, R. López-Medina and M. A. Bañares, *Catal. Lett.*, 2016, **146**, 1838–1847.
86 X. Lin, Y. Xi and J. Sun, *J. Phys. Chem. C*, 2012, **116**, 3503–3516.
87 Y. Li and J. N. Armor, *J. Catal.*, 1998, **173**, 511–518.
88 R. Bulánek, K. Novoveská and B. Wichterlová, *Appl. Catal., A*, 2002, **235**, 181–191.
89 S. Essid, F. Ayari, R. Bulánek, J. Vaculík, M. Mhamdi, G. Delahay and A. Ghorbel, *Solid State Sci.*, 2019, **93**, 13–23.
90 X. Liu, T. Liang, R. Barbosa, G. Chen, H. Toghiani and Y. Xiang, *ACS Omega*, 2020, **5**, 1669–1678.
91 T. Liang, X. Liu, Y. He, R. Barbosa, G. Chen, W. Fan and Y. Xiang, *Appl. Catal., A*, 2021, **610**, 117942.
92 G. Chen, T. Liang, P. Yoo, S. Fadaeerayeni, E. Sarnello, T. Li, P. Liao and Y. Xiang, *ACS Catal.*, 2021, **11**, 7987–7995.
93 W. L. Fierce and W. J. Sandner, *US Pat.*, 3028413, 1962.
94 P. F. Britt, *Pyrolysis and Combustion of Acetonitrile (CH_3CN)*, United States, 2002.

 This journal is © The Royal Society of Chemistry 2023

Published on 22 February 2023. Downloaded by Yunnan University on 8/24/2025 1:45:34 PM.

95 B. Venu, B. Vishali, G. Naresh, V. V. Kumar, M. Sudhakar, R. Kishore, J. Beltramini, M. Konarova and A. Venugopal, *Catal. Sci. Technol.*, 2016, **6**, 8055–8062.
96 J. S. J. Hargreaves, *Coord. Chem. Rev.*, 2013, **257**, 2015–2031.
97 L. Li, X. Mu, W. Liu, X. Kong, S. Fan, Z. Mi and C. J. Li, *Angew. Chem., Int. Ed.*, 2014, **53**, 14106–14109.
98 K. Dutta, V. Chaudhari, C.-J. Li and J. Kopyscinski, *Appl. Catal., A*, 2020, **595**, 117430.
99 L. Zhang, Z.-Y. Wang, J. Song, Y. Lang, J.-G. Chen, Q.-X. Luo, Z.-H. He, K. Wang, Z.-W. Liu and Z.-T. Liu, *J. CO_2 Util.*, 2020, **38**, 306–313.
100 K. Trangwachirachai, C.-H. Chen and Y.-C. Lin, *Mol. Catal.*, 2021, **516**, 111961.
101 K. Trangwachirachai, C.-H. Chen, A.-L. Huang, J.-F. Lee, C.-L. Chen and Y.-C. Lin, *Catal. Sci. Technol.*, 2022, **12**, 320–331.
102 Y. Zhang, T. Ma and J. Zhao, *J. Catal.*, 2014, **313**, 92–103.
103 M. O. Guerrero-Pérez and M. A. Bañares, *Catal. Today*, 2015, **239**, 25–30.
104 A. Ausavasukhi and T. Sooknoi, *Catal. Commun.*, 2014, **45**, 63–68.
105 N. M. Phadke, J. Van der Mynsbrugge, E. Mansoor, A. B. Getsoian, M. Head-Gordon and A. T. Bell, *ACS Catal.*, 2018, **8**, 6106–6126.
106 P. A. Holman, D. R. Shonnard and J. H. Holles, *Ind. Eng. Chem. Res.*, 2009, **48**, 6668–6674.
107 D. Cespi, F. Passarini, E. Neri, I. Vassura, L. Ciacci and F. Cavani, *J. Cleaner Prod.*, 2014, **69**, 17–25.